# Performance of 'first-article' scintillating fibres for the GlueX Barrel Calorimeter

B. Giesbrecht, A. Heinrichs, K. Janzen, S. Krueger, B. Leverington, G. Lolos, Z. Papandreou *, A. Semenov, I. Semenova, L. Sichello

*Department of Physics, University of Regina, Regina, SK, S4S 0A2, Canada*

E. Smith, B. Zihlmann

*Thomas Jefferson Accelerator Facility, Newport News, VA, 23606, USA*

**Abstract**

The response of reference-standard or 'first-article' Kuraray SCSF-78MJ (blue-green) scintillating fibres was measured by several methods, at Regina and Jefferson Laboratory. Firstly, by employing a 373-nm UV LED to stimulate the fibres along their length and reading out the light alternatively using a spectrophotometer and a photodiode. These yielded, respectively, the spectral response and the effective attenuation length from the photodiode's current readout. Secondly, by exciting the fibres using a $^{90}Sr$ radioactive source located at different measuring stations that allowed the extraction of the number of photoelectrons using vacuum photomultipliers as the photo sensors. Thirdly, diameter uniformity measurements were carried out. The results of all tests confirm that the fibres meet the GlueX specifications as contracted to Kuraray and, therefore, signal the start of production of fibres towards the construction of the GlueX Barrel Calorimeter. Finally, the Regina results set the reference standard towards fibre quality assurance during the production phase.

*Key words:* scintillating fibres, wavelength response, photoelectrons, attenuation length, electromagnetic calorimeter
*PACS:* 29.40.Mc, 29.40.Vj

* Corresponding author. Tel.: +1 306 585 5379; fax: +1 306 585 5659
*Email address:* zisis@uregina.ca (Z. Papandreou).

## 1 Executive Summary and Reference Standard for Production

The GlueX electromagnetic Barrel Calorimeter BCAL will be comprised of nearly 780,000 scintillating fibres. After a bidding process, the fibre contract was awarded by Jefferson Lab (JLab) to Kuraray [1]. A condition of the contract was for Kuraray to deliver 50 "first-article" fibres to JLab and another 50 to Regina, while holding on to a third set of 50. All fibres were extracted from one preform and tested by Kuraray before shipped to JLab and Regina.

The objective of the study herein is to examine the principal characteristics of Kuraray SCSF-78MJ scintillating optical fibres, namely the uniformity in diameter, the produced spectral shape, the effective attenuation length, and the light output in terms of the number of photoelectrons measured [1]. The contract specifications to Kuraray and test results are summarized below. As evaluation of the production fibres will be carried out exclusively at Regina, only the Regina results are shown on this page and these will form the reference standard for fibre quality assurance during the production phase.

- **Diameter.** *Specifications:* Dimensional uniformity of the diameter was specified at 1 mm with $RMS \leq 2\%$. *Measurements:* The diameter was measured at three lengths across each fibre (50 cm, 200 cm and 350 cm) and was found to be $(1.002 \pm 0.006)$ mm with $RMS \leq 0.6\%$.
- **Spectral shape.** The spectral shape was measured using a spectrophotometer and was as expected, based on past measurements and experience of similar types of fibres.
- **Effective attenuation length.** *Specifications:* greater than 300 cm when measured with a bi-alkali photomultiplier tube and with $RMS \leq 10\%$. *Measurements:* The effective attenuation length was extracted by fitting over the 100-280 cm source distance range with a single exponential function, and was found to be $(351 \pm 17)$ cm with $RMS \leq 5\%$ using a photodiode and having the far fibre end polished and blackened.
- **Light output.** *Specifications:* This is quantified by the GlueX Collaboration as the number of photoelectrons collected at the fibre's end and must be greater than 3.5 p.e. using a bi-alkali PMT at 200 cm from the source and with $RMS \leq 15\%$. *Measurements:* The mean extracted number of photoelectrons at 200 cm was found to be $7.1 \pm 0.7(stat) + 0.7(syst)$ with $RMS < 10\%$, by employing a standard bi-alkali vacuum PMT.

The tested fibre samples meet or exceed the contract specifications to Kuraray. A few damaged fibres were observed, possibly due to handling in Regina during the initial stages of experimental setup refinements.

[1] Other parameters were cladding thickness, time structure of the scintillation light and base material components, but these were not evaluated and thus not reported herein.

## 2 Introduction

The study in this paper was undertaken in the context of determining whether the SCSF-78MJ scintillating fibres provided by Kuraray to GlueX [1] meet the specifications as layed out in the contract. Specifically, the key parameters tested and reported herein are a) dimensional uniformity (diameter of 1 mm with a $RMS \leq 2\%$), b) spectral response (wavelength of maximum emission between 450-500 nm), c) the effective attenuation length, $\xi$, (greater than 300 cm when measured with a bi-alkali photomultiplier tube - PMT and with $RMS \leq 10\%$), and d) the light output, quantified as the number of photoelectrons, $\zeta$, collected at the fibre's end) greater than 3.5 p.e. using a bi-alkali PMT at 200 cm from the source and with $RMS \leq 15\%$). Other parameters were cladding thickness, time structure of the scintillation light, and base material chemistry, but these were not evaluated and thus not reported herein.

To this end, Kuraray produced two preforms and the first was used to extract $55 \times 3$ canes of *standard reference fibres* for evaluation at Kuraray, JLab and Regina, respectively. One hundred of these fibres were sent to the latter two sites (50 each) and will be referred to as *first article* fibres herein. Because the Regina shipment (containing Lot 3) showed damage on the crate's exterior, it was deemed prudent to send 20 JLab fibres (Lot 2) to Regina and for JLab to keep 20 Regina fibres. In the end, after measurements, the crate damage did not seem to have affected the fibres inside. The final distribution of fibres at the two sites is shown in Table 1 below. Fibre labelling was established by Kuraray as $i - j$, with $i$ and $j$ being the lot and fibre numbers, respectively.

| **JLab Fibres** | **Regina Fibres** |
|---|---|
| $2-1 \div 2-10$ | $3-1 \div 3-10$ |
| $2-11 \div 2-20$ | $3-11 \div 3-20$ |
| $3-21 \div 3-30$ | $2-21 \div 2-30$ |
| $3-31 \div 3-40$ | $2-31 \div 2-40$ |
| $2-41 \div 2-50$ | $3-41 \div 3-50$ |

Table 1
The fibre lot distribution between JLab and Regina is tabulated.

Two distinct methods were employed at Regina towards the determination of the attenuation length and a third method was based on JLab data. Two methods were used to extract the number of photoelectrons. All methods will be expounded upon and compared to each other and to the measurements conducted by Kuraray.

## 3 Project Background

The production fibres are to be coupled to the electronic front-end readout of the electro-magnetic barrel calorimeter (BCAL) for the GlueX project [2,3]. The BCAL is a sampling calorimeter based on scintillating fibres and will be deployed inside the GlueX detector's super-conducting solenoid. The central field of the solenoid is 2.2 T, resulting in substantial magnetic field strength and gradients near the BCAL ends, so using vacuum PMT's with short light guides is not possible. Whatever the readout sensors turn out to be, it is important that the fibres yield the highest possible amount of light, measured by the sensor as photoelectrons, and to simultaneously have a long attenuation length considering the detector's length.

The BCAL will be comprised of a lead and scintillating fibre matrix, consisting of ∼190 layers of corrugated lead sheets, each of 0.5 mm thickness, and 1-mm-diameter, multi-clad, scintillating fibres (SciFi), bonded in place of the lead grooves using BC-600 optical epoxy [2] . This geometry results in ∼16 000 fibres per module. The detector will consist of 48 modules, each having a trapezoidal cross section (8.5-12.5 cm taper), and will form a 390 cm long cylindrical shell with inner and outer radii of 65 cm and 90 cm, respectively.

The chemical and optical properties of scintillating materials have been presented elsewhere [4–6]. Typical absorption and emission spectra and their relation to our UV LED can be found in our past work [7].

## 4 Uniformity in Diameter - Regina Measurements

The fibre diameter was measured at Regina, at three positions along the length of each fibre, namely, 50 cm, 200 cm and 350 cm, and was found to be (1.002±0.006) mm ($RMS \leq 0.6\%$) using a micrometer caliper. The results are plotted in histograms and shown together with the Kuraray measurements of eccentricity in Fig. 1. Note that the eccentricity, $\rho$, is defined by the following equation:

$$\rho(\%) = \frac{(d_{max} - d_{min})}{\frac{1}{2}(d_{max} + d_{min})} \times 100 \tag{1}$$

[2] St. Gobain Crystals & Detectors, Hiram, OH 44234, USA (www.bicron.com)

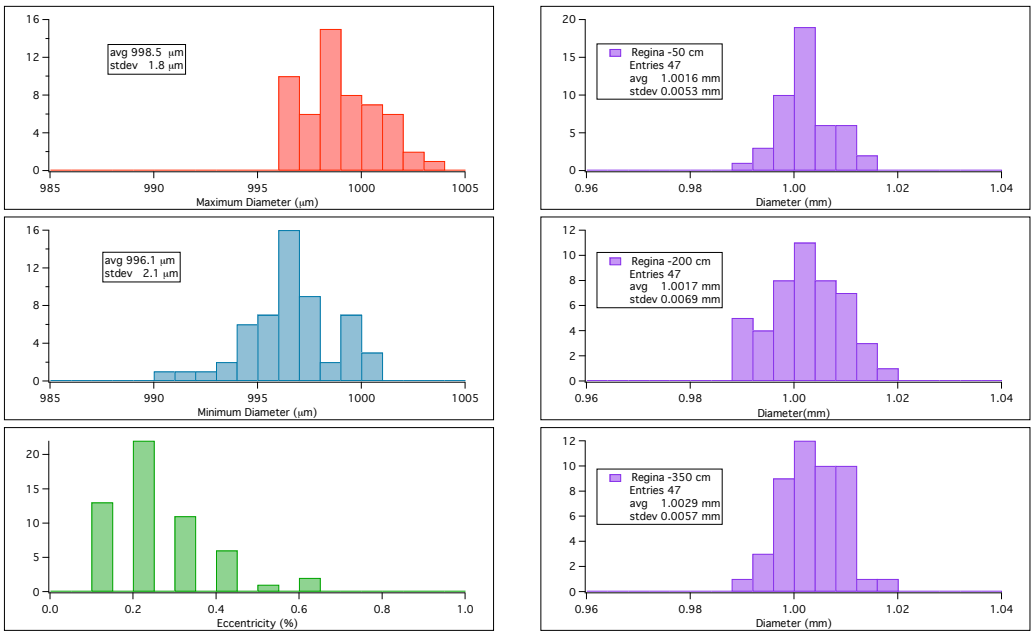


Fig. 1. *Left panel:* The Kuraray measurements of maximum and minimum diameter and eccentricity (out of round) are shown. *Right panel:* The uniformity of the fibre diameter, measured at Regina, is graphed at three positions along the length of each fibre.

## 5 Spectral Response - Regina Measurements

### *5.1 Experimental Setup*

For the measurements reported herein, a LED light source, a spectrophotometer and the tested SciFi were coupled together in a robust manner. The USB4000 single-channel fibre optic spectro-photometer [3] is based on a blazed diffraction grating with a 50 $\mu$m wide slit and features a high-sensitivity 3648-element linear CCD array that provides high response and excellent optical resolution from 200-1100 nm and a 16 bit A/D. This device had been calibrated by the manufacturer, and the provided specifications indicated a wavelength difference, $|\delta\lambda|$, between expected and measured values, never exceeding 0.3 nm for any given pixel on the CCD. The USB4000 connects to a PC running commercial software via a USB2.0 interface. The spectrophotometer has a maximum integration window of 3.8 ms and a resolution of $\sim$3.3 bins/nm (or 0.3 nm). The absolute intensity calibration of this device was unknown, as it was loaned to Regina for evaluation by Gamble Technologies [4]. However, this absence was deemed unimportant towards the extraction of the spectral

[3] Ocean Optics Inc., Dunedin, FL, USA (www.oceanoptics.com)
[4] Gamble Technologies, Mississauga, ON, L5N 2M2, Canada (www.gtl.ca)

shape and comparison to that advertised by Kuraray. Finally, past tests [7] had demonstrated that these spectro-photometers are correctly calibrated versus wavelength by their manufacturer and that there is no significant direct contribution from the light source to the intensity of the measured fibre spectra in the wavelength range of interest.

For our measurements, a RLS-UV380 ultra violet LED [5] was employed, with a peak emission wavelength of 380-385 nm and power dissipation of 60 mW.

Each fibre was first cleaned using ethyl alcohol and Kim wipes and was handled using white cotton gloves. The test fibre was then positioned horizontally in a 420-cm long 1-mm-deep channel, machined in a black poly-ethylene bar ("puck board" material), that had a measuring scale attached to one of its long sides.

The first (fibre cane 2-33) test fibre's end was successively rough cut near its tagged end, polished and blackened using black mat enamel paint (used for scale model painting). Measurements were taken at all three configurations and showed that the bulk attenuation behaved as expected, resulting in the blackened end having the lowest value due to elimination of reflections. From then on, the far end of all fibres was polished and blackened. Details are provided in Appendix B.1.

The near end of the fibre was polished using a Fibre Fin 4 diamond polisher [6] and then threaded through a BFA-SMA connector mounted on an Ocean Optics BFA-KIT custom chuck, that allowed the fibre's end to be placed flush with the SMA end, while held in place with a rubber-lined clamp. The SMA end was connected to the USB4000 input. In its interior lies a short-length fibre that illuminates the CCD via a series of lenses and mirrors, while its other end is placed in direct contact with the Kuraray test fibre with an air gap between them.

This method allowed for fast and easy coupling of fibre to spectrophotometer. The setup was made robust to protect against displacing the test fibre and was leveled to avoid any curvature in the test fibres. Despite these precautions, the fibre would "lift" from its groove occasionally, requiring the measurement to be repeated. Following the "first article" tests, an optical diffuser was installed between the LED and fiber and this "stabilized" the data as the setup became considerably less sensitive to fiber placement. Details will be provided in a subsequent report on the production fibre performance [8].

Although the coupling reproducibility varied in the aforementioned setup, this effect does not influence the extracted spectral shape nor the attenuation length but rather only the absolute light output. The attenuation length could

[5] Roithner Lasertechnik,Vienna, Austria (www.roithner-laser.com)
[6] FibreFin Inc. 201 Beaver Street, Yorkville, IL 60560 USA

be extracted using the spectrophotometer and position scans, but in the end a more expedient method was employed, based on a photodiode. The light output was studied at a separate measuring station, using a photomultiplier. Both techniques are reported below.

The LED was installed in a commercial housing and was mounted on a custom-design fixture that could slide on the lab bench guided by the puck board, and translated across the length of the fibre (from 10 cm to 400 cm in 10 cm steps). The distance of the LED to each fibre tested was held constant to maintain a consistent beam profile; however, the resulting profile was narrow (prior to the installation of the optical diffuser) and may have resulted in a small non-uniform illumination of the fibre at different positions along its length, owing to the manner in which the mount "fit" across the puck board. This effect and the fibre coupling reproducibility mean that absolute comparisons of the measured intensity from one fibre to another were not possible. Nevertheless, relative comparisons of the measured light intensity along the length of a given fibre were possible, since the spectral shapes and effective attenuation are insensitive to these non-uniformities and could be extracted reliably.

All measurements were carried out in near darkness in our lab, employing small desk lamps to provide ambient light. However, since the core of blue-emitting scintillating fibres can be damaged by prolonged exposure to UV light, yellow, UV-absorbing film (TA-81-XSR [7]) was used to cover all overhead fluorescent lights and the desk lamps during the preparation and setup stages. The resulting light spectra were confined to wavelengths above 450 nm and thus above the damaging UV range. Details will be reported in reference [8].

### *5.2 Results*

Wavelength spectra at 10 cm, 30 cm, 100 cm and 300 cm from fibre 3-6 are shown in Fig. 2, together with the corresponding Kuraray spectra from their 2007 scintillation material brochure [10]. The peak intensity and the integrated spectral strength scale as a function of distance from the light source in a similar manner for both sets of measurements. Although the two sets are qualitatively similar, there are differences in the exact spectral shapes owing perhaps to the different dyes used by Kuraray's supplier in the first-article fibres and their past work (2007). The first-article spectral response data has been requested from Kuraray, and when received this issue will be revisited. The different measuring techniques and the specific choice of fibre tested at Regina may also contribute, although probably to a lesser extent.

[7] Window Film Systems, London, ON, Canada (www.windowfilmsystems.com)

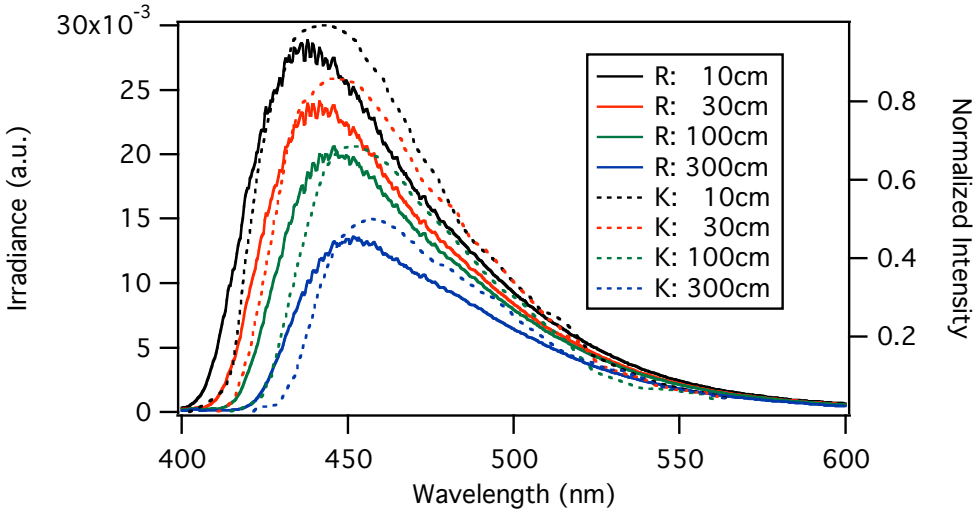


Fig. 2. Wavelength spectra, measured at Regina, at source distances of 10 cm, 30 cm, 100 cm and 300 cm from fibre 3-6 are shown in Fig. 2 as solid lines, together with the corresponding Kuraray spectra [10] displayed as dotted curves. The former are irradiance measurements, and the y-axis maximum for the latter has been set to 1.

## 6 Attenuation length using a photodiode - Regina Measurements

The spectrophotometer method is useful in examining the fibre wavelength response but a more expedient method was employed based on a Hamamatsu calibrated S2281 photodiode in order to extract the attenuation length. (Note: the "calibrated" feature of this device was not needed and therefore not employed in these tests.)

### *6.1 Experimental setup*

Each tested fibre was handled and positioned on the "puck board" as detailed in Section 5. The spectrophotometer was replaced with the photodiode, which was attached via clamps to a laboratory stand through which the fibre was threaded. The polished end of the fibre was coupled to the photodiode using Dow Corning [8] optical grease, whereas the other end was polished and blackened, as reported previously. The attenuation length of selected fibres was also extracted based on different treatment of the ends and is reported in Appendix B.1.

[8] Dow Corning Corporation, Midland, 48686 MI, USA (www.dowcorning.com)

The S2281 was read out initially using a Keithley 617 Electrometer [9]. This device was used to measure the first 26 fibres. Subsequently, our group purchased a Keithley 6485 picoammeter, dedicated to all fibre tests, starting with select re-measurements of first article fibres and continuing with the first shipment of production fibres [8]. Several comparisons of the devices were carried out using the same and different fibres and all yielded consistent results, once accounting for the fibre coupling was made. The Keithley 6485 was used to measure another 17 first-article fibres, for a total of 43 out of the 50 fibres. Four fibres were damaged, most likely due to initial handling in Regina, as reported in Appendix A. The remaining three fibres were not tested.

### *6.2 Results*

Following all checks in Section B.1, data were collected from 43 of the first article fibres at Regina, with the near end always polished and coupled with optical grease to the S2281 photodiode, and the far end always polished and blackened. The results are shown in Section 8. The Regina photodiode measurements yielded $\xi = (351 \pm 17)$ cm whereas the Kuraray result was $\xi = (374 \pm 17)$ cm.

## 7 Number of photoelectrons

### *7.1 Regina Measurements*

#### *7.1.1 Experimental setup*

Fibre 2-29 had both ends polished and was inserted in a dedicated measuring station contained in a 4.5-m-long dark box. One fibre end was coupled to a Hamamatsu R329-02 calibrated photomultiplier, with a standard R329-02 progressive voltage divider, and the other to a SensL [10] silicon photomultipier (SiPM) having a $3 \times 3$ mm active area and based on their A20HD microcell. This particular SiPM had been previously calibrated with respect to its photon detection efficiency (PDE) versus a calibrated Hamamatsu photodiode when the scintillation light was provided by a Kuraray SCSF-78MJ fibre excited by a 375 nm laser [11]. The SiPM was operated at an overbias of +2 V; there, its PDE was measured to be 7.2%. The PMT High voltage was set to 2200 V. Both fibre ends were coupled using optical grease.

[9] Keithley Instruments, Inc., Cleveland, 44139 OH, USA (www.keitlhey.com)
[10] SensL, Blackrock, Cork, Ireland (www.sensl.com)

For these tests, a $^{90}Sr$ radioactive source, placed within a custom-designed Pb collimator, was located over the near centre point of the fibre and approximately 200 cm from the SiPM end. The collimator consisted of a $4 \times 4$ cm$^2$ Pb block, having an 8 mm diameter partial bore to house the source, located above a slit ($13\ (h) \times 0.5\ (w) \times 8\ (l)$ mm$^3$) and a $1 \times 1$ mm$^2$ cutout along the bottom of the collimator for fibre illumination and placement, the cutout being parallel to the 8 mm slit side. The collimator was designed carefully and included a lid, since it was determined that a small amount of "backsplash" activity resulted from source electrons striking the lid of the black box.

A small ∼9 cm-long scintillator counter was coupled to a Burle 8575 PMT (HV at 1700 V) and was placed directly below the fibre, which was thus sandwiched between the source/collimator and small counter. The latter counter provided the trigger for the data acquisition, and fired at a rate of approximately 1 KHz. The experimental setup is sketched in Fig. 3.

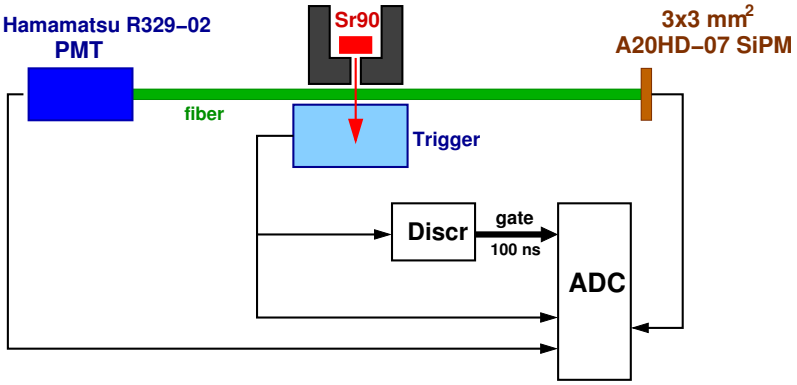


Fig. 3. The setup used to measure the number of photoelectrons from the first article fibres is sketched here. Although not shown in this schematic, the Pb collimator containing the $^{90}Sr$ radioactive source had a Pb lid during data taking.

Care was exercised in setting of the discriminator threshold. Measurements were also taken with the $^{90}Sr$ removed, with the SiPM disconnected and with the source and trigger counter moved away from the fibre in order to determine the SiPM pedestal and the random triggers, the latter being indeed random with an accuracy better than 1%. These efforts aimed at producing a data set that suppressed experimental or analysis bias. The unambiguousness in extracting the number of photoelectrons arriving at both the SiPM and Hamamatsu PMT is portrayed in Fig. 4. The few background events leaking through the system are visible as a narrow red line parallel to the SiPM ADC axis and at 27 ADC units on the PMT ADC axis.

### *7.1.2 Analysis Method*

The collected SiPM ADC spectra prominently displayed individual photoelectron peaks, sometimes clearly visible up to 16 in number. Subsequently, the

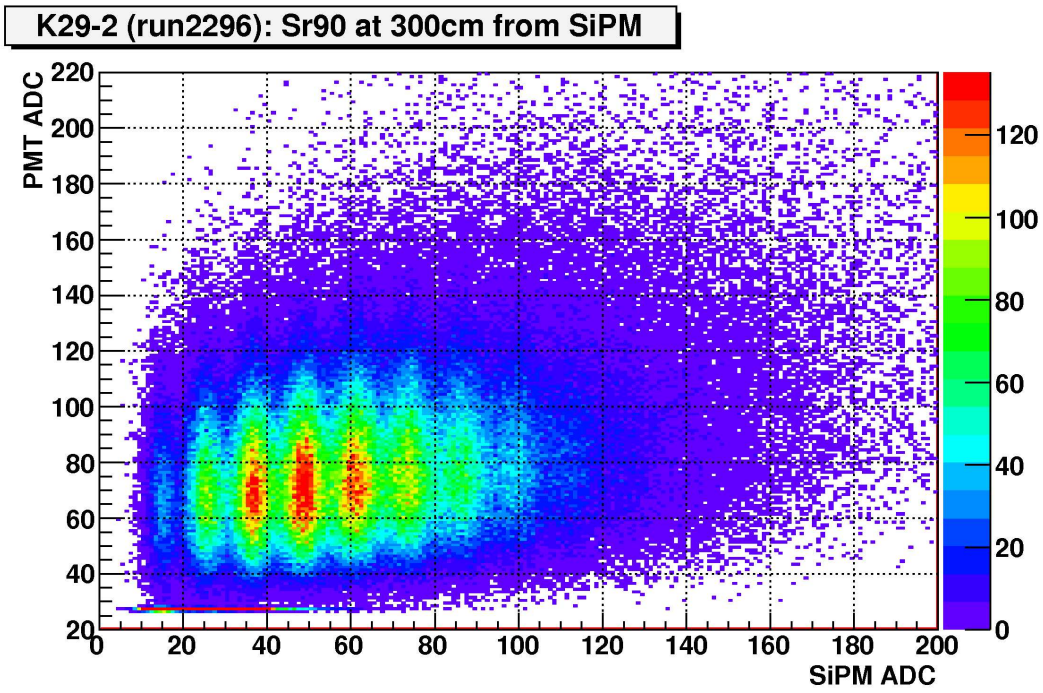


Fig. 4. The amplitude of the SiPM versus that of the Hamamatsu PMT is shown in units of ADC with the source at 300 cm from the SiPM, i.e. approximately 100 cm from the PMT. The SiPM photoelectron bands are clearly visible and the background-related pedestal in the PMT (red-coloured, horizontal line at approximately 27 ADC units on the y-axis) is also clearly separable from the SiPM-correlated signal.

$^{90}Sr$ source and trigger counter were positioned at several locations along the length of the fibre, keeping their respective geometry fixed. The resulting SiPM spectra from three positions are shown in Fig. 5. Clear separation of photoelectron peaks in the ADC spectra from the SiPM allows us to fit the ADC spectra to the function that is the sum of Gaussian peaks; the number of events in each of $i$-photoelectron peaks, $A_i^s$, can be found from the amplitude and width of the correspondent Gaussian peak, and the average number of photoelectrons can be extracted via the formula:

$$N_{pe} = \frac{1}{A_s}\sum_i (i\,A_i^s) - \frac{1}{A_p}\sum_i (i\,A_i^p), \tag{2}$$

where $A_s = \sum A_i^s$ is the total number of events in the $^{90}Sr$ spectrum. The second term in the equation addresses the contribution of the non-negligible SiPM noise; the total number of "pedestal" events $A_i^p$ and the number of events for each of $i$-photoelectron peaks $A_i^p$ can be extracted from the fit of pedestal ADC spectrum for SiPM (viz., the bias voltage is applied to SiPM but the $^{90}Sr$ source is removed). A sample pedestal spectrum is displayed in the bottom right panel of Fig. 5, taken over a period of approximately 14 hours.

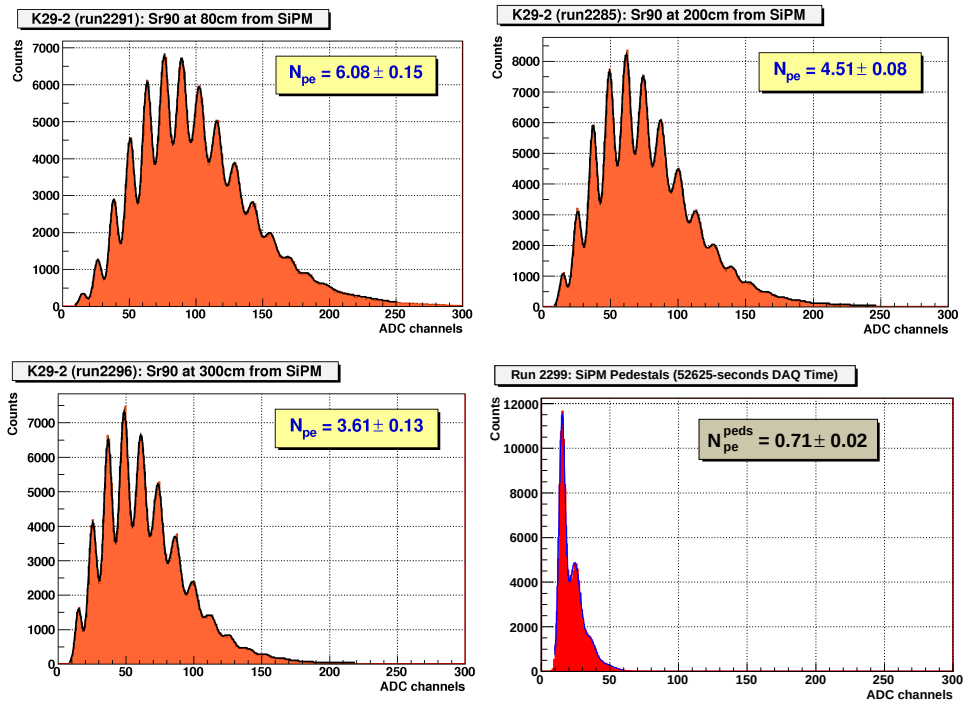


Fig. 5. The number of photoelectrons as measured by the SiPM is shown for three different positions of the $^{90}Sr$ source and trigger counter. The bottom right panel shows a pedestal run taken with electrons from the $^{90}Sr$ source striking the trigger counter while displaced from the fibre that remained connected to the SiPM.

It should be noted that the number of photoelectrons shown in that panel has already been subtracted from the other three panels in this figure, yielding the final number in each. Once the pedestal spectra had been normalized for the data acquisition time, they amounted to a 1% subtraction as outlined above.

Following the above proof of principle tests using fibre 2-29, the SiPM electronics board ceased functioning. While waiting for replacement boards, it was decided to measure the photoelectrons from the first article fibres using the Hamamatsu PMT.

The widths of the observed ADC spectra from the PMT are the result of both the fluctuations in the number of photoelectons and the variations in the enegry deposited in the fiber. To address this extra-broadening of the spectra, we simulated the energy deposition from the electrons in the realistic model of the measurement setup using FLUKA 2008.3 program [12]. The simulated Birks-corrected energy depositions in the fibre were recorded on event-by-event basis. The resulting spectrum $F(\Delta E)$ of energy deposited in the fiber by electrons is shown in Fig 6; mean energy depositions $\overline{\Delta E}$ were calculated. Using the simulated $F(\Delta E)$ functions, we fit experimental pedestal-subtracted ADC spectra from PMT to the function (red line in Fig. 7):

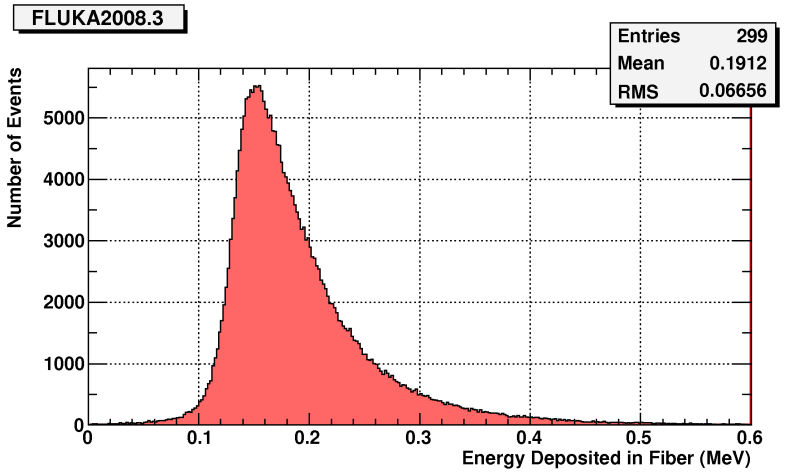


Fig. 6. The distribution of the energy deposition due to the $^{90}Sr$ source in a fibre is shown, as simulated using the Monte Carlo package FLUKA 2008.3. The simulated mean energy deposition was ∼0.19 MeV/fibre, corresponding to traversal of $\beta$s from the $^{90}Sr/^{90}Y$ mother/daughter pair, past the collimator and through the 1-mm fibre.

$$f(x) \sim \int_{E_{min}}^{E_{max}} d(\Delta E) \left[ F(\Delta E) \cdot \sum_{n=0}^{n_{max}} Poi(n,\, k \cdot \Delta E) \cdot Gau(x, n, \sigma_n) \right], \quad (3)$$

where $Poi(n,\, k \cdot \Delta E)$ is the Poisson distribution with the expected value of $(k \cdot \Delta E)$, $k = (N_{pe}/\overline{\Delta E})$ is energy-to-NPE conversion factor, $Gau(x, n, \sigma_n)$ is the Normal distribution with the mean value of $n$ and standard deviation of $\sigma_n$. The counter $n_{max}$ truncates the infinite series in the summation and was chosen to lie comfortably higher than the largest number of photoelectron peaks. We estimated the value of PMT gain resolution $\sigma_n$ for $n$ photoelectrons using the formula (see [13,14]):

$$\sigma_n^2 \;=\; n\frac{g^m - 1}{g^m(g-1)} \;\approx\; n\frac{1}{g-1}, \quad (4)$$

where $g$ is the mean dynode secondary emission coefficient (in our case, about 4.0) determined from the gain of the PMT (see Fig. 7), and $m = 12$ is the number of dynodes in the PMT. Typical three-parameter ($N_{pe}$, ADC channel corresponding to $N_{pe}$ and y-scale) fits to the ADC spectra from PMT are also shown in Fig. 7 as red lines. This method was subsequently applied to the SiPM data – with the addition of a fourth parameter describing the photoelectron peak width – and yielded a consistent number of photoelectrons within error.

A strong correlation between mean amplitudes (averaged on run-by-run basis) and corresponding extracted mean numbers of photoelectrons is plotted in Fig. 7, as expected. Finally, the attenuation length was extracted for fibre 2-29

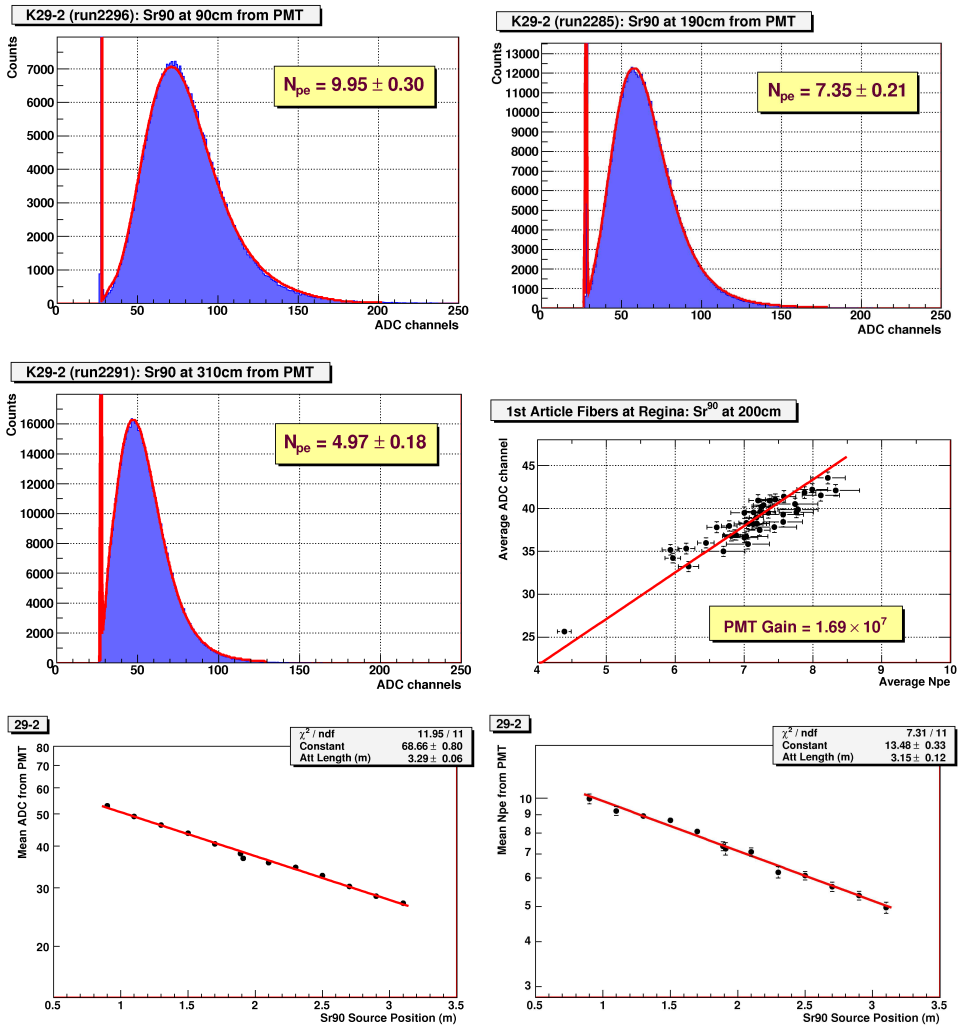


Fig. 7. Three fits to the PMT ADC spectra are shown, for source positions of 90 cm, 190 cm and 310 cm, and the resulting mean number photoelectrons is shown in the insets. The correlation between the mean PMT amplitudes and mean number of photoelectrons is depicted in the right panel of the middle row and the slope of this graph yields the PMT's gain, using a progressive voltage divider. The attenuation length extracted from the PMT ADC's mean and the mean number of photoelectrons are portrayed in the left and right panels of the bottom row, respectively.

both from the mean ADC amplitudes and mean numbers of photoelectrons, as shown in the bottom row of Fig. 7. The two methods yielded consistent results within $1.5\sigma$ of $\xi = (329 \pm 6)$ cm and $(315 \pm 12)$ cm, respectively. Examining the values alone, the small systematic difference may be due to a non-linearity in the ADC, particularly at low channel numbers, that could be removed following a dedicated calibration procedure.

In order to verify the analysis technique used for the extraction of $N_{pe}$, the PMT gain extracted from our $N_{pe}$ measurements was compared to the gain calibration curve for this PMT measured by Hamamatsu personnel as a ratio

of anode and photocathode currents. The PMT gain ($g_{PMT}$) was derived from the ratio of a PMT anode charge ($Q_{anode}$) measured with the ADC and the number of photoelectrons extracted using the aforementioned technique:

$$g \;=\; Q_{anode}/(e \cdot N_{pe}) = (2 \cdot ADC \cdot \alpha)/(e \cdot N_{pe}) \qquad (5)$$

where $ADC$ is an average value for ADC spectrum of PMT, $\alpha = 0.25$ pC/ch is the input sensitivity of LeCroy 2249A ADC we used, $e$ is the charge of electron, and the factor 2 in the nominator of the ratio reflects the fact that ADC (with 50-Ω input impedance) sees only a half of PMT anode charge because of the employed 50-Ω termination on the PMT divider. To be consistent with conditions of R329-02 PMT calibration made by Hamamatsu, for these measurements a Hamamatsu-recommended "linear" HV divider was used with the ratio of voltage drops between the dynodes of 4:1:1.4:1: ... :1. The PMT gain results obtained with three different fibers as a function of HV supply voltage are shown in Fig. 8 as blue open circles, and are in a good agreement with the calibration curve (red line) from Hamamatsu. The small (∼10%) discrepancy is most likely due to small mismatch between the ADC impedance and 50-Ω termination on the divider as well as on the non-linearity of low channels of ADC scale, and it effectively translates to an underestimation of $N_{pe}$.

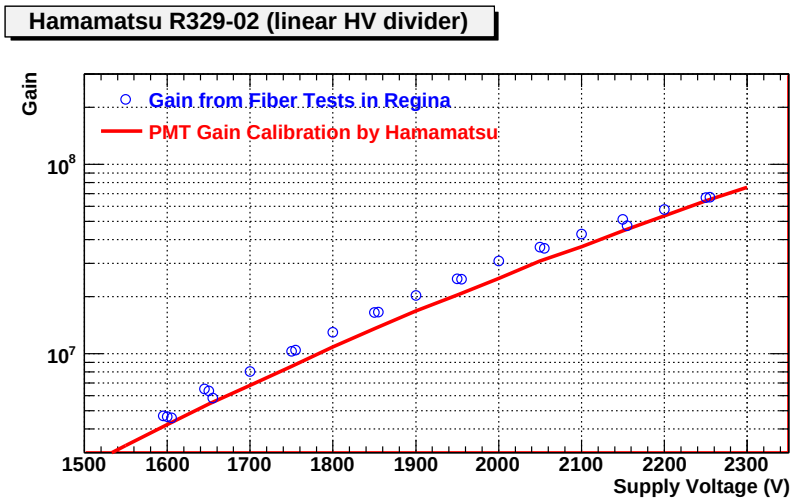


Fig. 8. The gain of the R329-02 PMT is plotted as a function of applied high voltage and compared to Hamamatsu's gain calibration of this PMT.

### *7.1.3 Results*

Once the data-taking and analysis procedures were firmly established, 43 of the fibres – measured at the attenuation length station using the photodiode – were transferred to the photoelectron measuring station. There, the number of photoelectrons resulting from the $^{90}Sr$ radioactive source excitation of the fibre's core material was extracted, using the PMT as the photosensor. The

results are graphed in Fig. 9 and yield a mean extracted number of photoelectrons $\zeta = 7.1 \pm 0.7$ at 200 cm from the radioactive source, well exceeding the contract specifications of greater than 3.5 with an RMS of 15%. Three broken fibres (3-3, 3-9 and 3-49) were removed from the data set; see details in Section A.

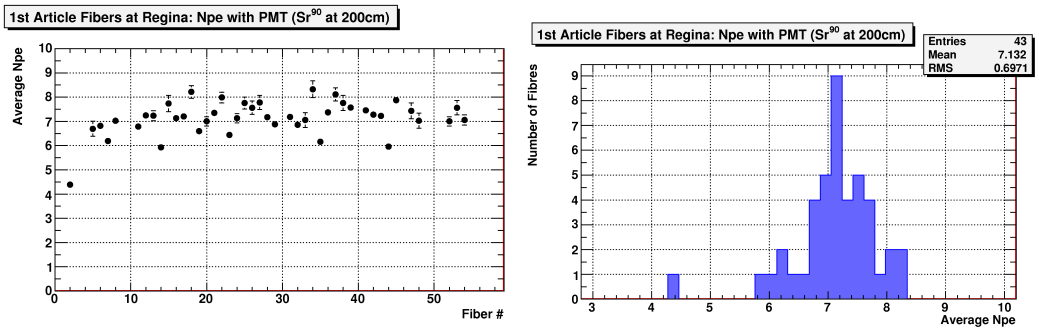


Fig. 9. The mean number of photoelectrons from 43 Kuraray first article fibres at Regina, is shown versus fibre number (left) and as a histogram (right).

## *7.2 JLab Measurements*

### *7.2.1 Experimental setup*

Each 410 cm long fibre was inserted in a dark box above a linear slide with a moving table. A copper collimator with a 1 mm groove in which the fibre was placed, was positioned on the table. The table and collimator move along the fibre's length. Above the groove, but in the center, a 0.5 mm wide slit was cut through the collimator material. The slit is 2 mm or 5 mm long depending on which collimator was used; for the final measurements the larger slit was used. The general setup is depicted in Fig. 10. The electrons from the $^{90}Sr$ source pass through the collimator slit through the fibre and finally into the trigger scintillator (TPM). The data acquisition (DAQ) receives the trigger from the TPM to digitize the signals from all detectors including the XP1911 (FPM) a 1" PMT that is coupled to one end of the fibre with mechanical contact between the PMT glass and the fibre without optical grease.

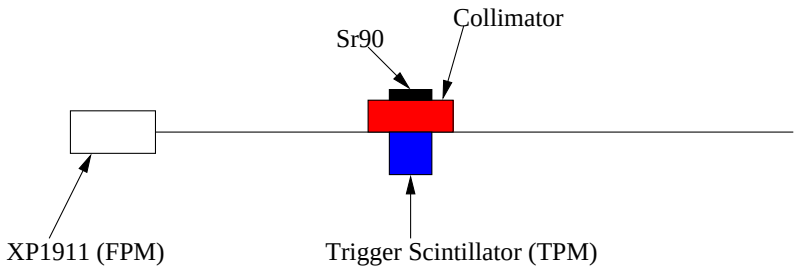


Fig. 10. General sketch of the fibre test setup at JLab.

The signal from the FPM was amplified by a factor of 10 before multiplexed using a linear fan in/out based on NIM electronics. The linear fan in/out allows the adjustment of the DC signal offset in such a way that the resulting pedestal can be set above the built in pedestal threshold of the charge integrating ADC, a VME-based 16 channel ADC from CAEN V792N. The integration length of the ADC gate was set to 63 ns, sufficient to contain the full signal from the PMTs. Because only a few photo electrons are expected to be seen by the FPM, the signal will be small. The total charge from a signal caused by a single photo electron will be well below 5 pC, which is the average built in pedestal of the ADC. To keep the signal amplification at reasonable values a negative DC offset was added to the analog signal to make sure that the integrated charge is always above 5 pC. This also means that the width of the pedestal directly reflects the noise in the system.

The fibre end coupled to the FPM was polished using a Fiber Fin 4 device. The other end of the fibre was not treated – in contrast to the Regina tests – and left as was received from Kuraray for all measurements except a few: tests were carried out to investigate the effect of treating the other end, in particular by painting it black, polishing it or applying both treatments, and these are reported below.

Data are recorded using a $^{90}Sr$ source with a intensity of 25 $\mu$Ci. The source-collimator-TPM assembly was moved along the fibre in steps for 10 cm from 50 cm to 320 cm. This was done with a remote controlled motor that drives the linear slide on which the collimator is located. At each position data were taken for 10 minutes. Additional tests were carried out to understand the results in terms of the measurement conditions, in a fashion similar to those reported in Section B.1. Specifically, the opposite fibre end was just polished, just painted, and polished and painted. The results are shown in Appendix B.2.

### *7.3 Results*

Thirty eight fibres were measured and the mean number of photo electrons and attenuation length determined. The analysis of the ADC spectra was carried out as described above in Section 7.1.2. A typical fitted ADC spectrum and the extracted gain for the XP1911 PMT are shown in Fig.11.

The attenuation length was extracted, alternatively, by fitting a single exponential to the mean number of photoelectrons and the mean ADC value from the PMT as a function of source distance from the PMT, both in the 100-280 cm range. As an example, the extracted attenuation lengths for fibre 2-29 were $(377 \pm 7)$ cm and $(351 \pm 7)$, respectively. These two quantities track linearly with respect to each other as expected and are also shown in Fig. 11.

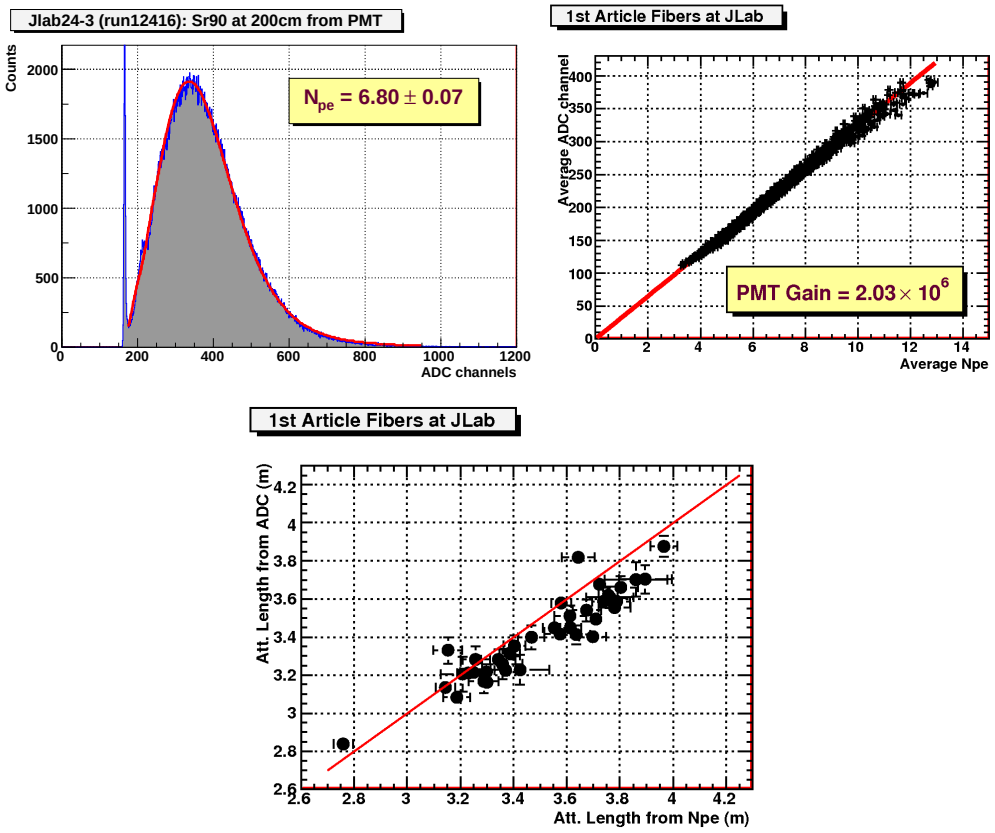


Fig. 11. *Top left:* A sample fit of the JLab ADC is shown for fibre 3-24 with the $^{90}Sr$ positioned at 200 cm from the XP1911 PMT. *Top right:* The average ADC channel is plotted versus the extracted number of photoelectrons. The slope provides the PMT's gain. *Bottom:* The attenuation lengths extracted from the mean ADC channel and the mean number of photoelectrons are plotted against each other, extracted from single exponential fits in the 100-280 cm source distance range. The errors are statistical. A strong linear correlation is observed as expected, lending support to the analysis method. The 45° red line in the bottom panel represents the line of equal attenuation length values from the two extraction methods.

The JLab data are summarized in Fig. 12. The attenuation length results are grouped in Fig. 13 together with the Kuraray and Regina results.

## 8 Comparisons and Discussion

### *8.1 Attenuation Length*

The three data sets are plotted in histogram fashion in Fig. 13, extracted from single exponential fits in the 100-280 cm source distance range. The reader is reminded that Regina had the far fibre end polished and blackened, whereas

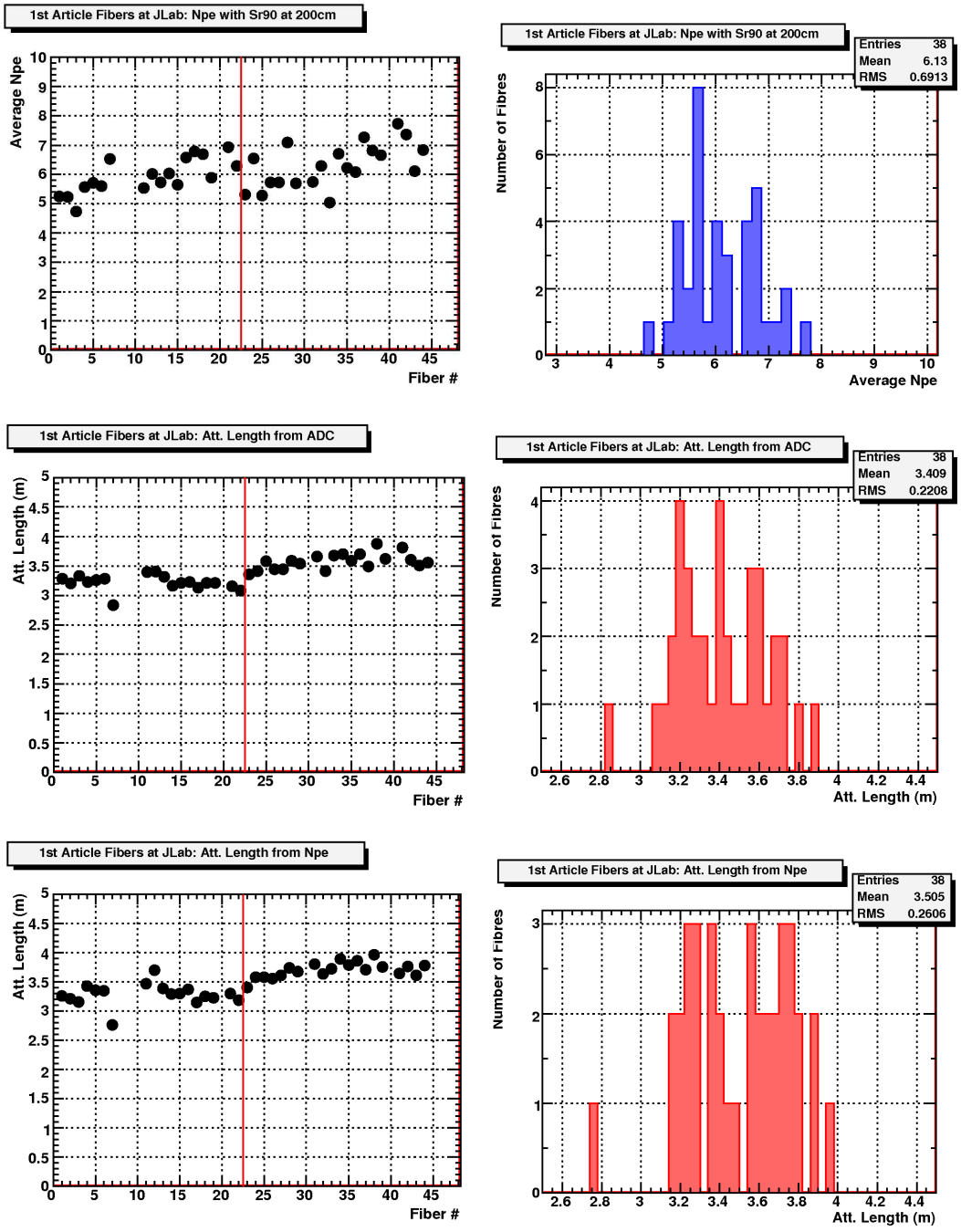


Fig. 12. Summary of JLab results. The panels are self explanatory. The vertical red line indicates the cross over from fibre Lot 2 to Lot 3, as mentioned in Section 2.

JLab left it a rough cut. Kuraray carried out measurements for both end configurations, but here the opposite end blackened ones are shown.

The Regina photodiode-based measurements yielded (351±17) cm whereas the JLab PMT-based tests resulted in $(351 \pm 26)$ cm and $(341 \pm 22)$ cm, based on $N_{pe}$ and the mean ADC value, respectively. The Kuraray PMT-based result

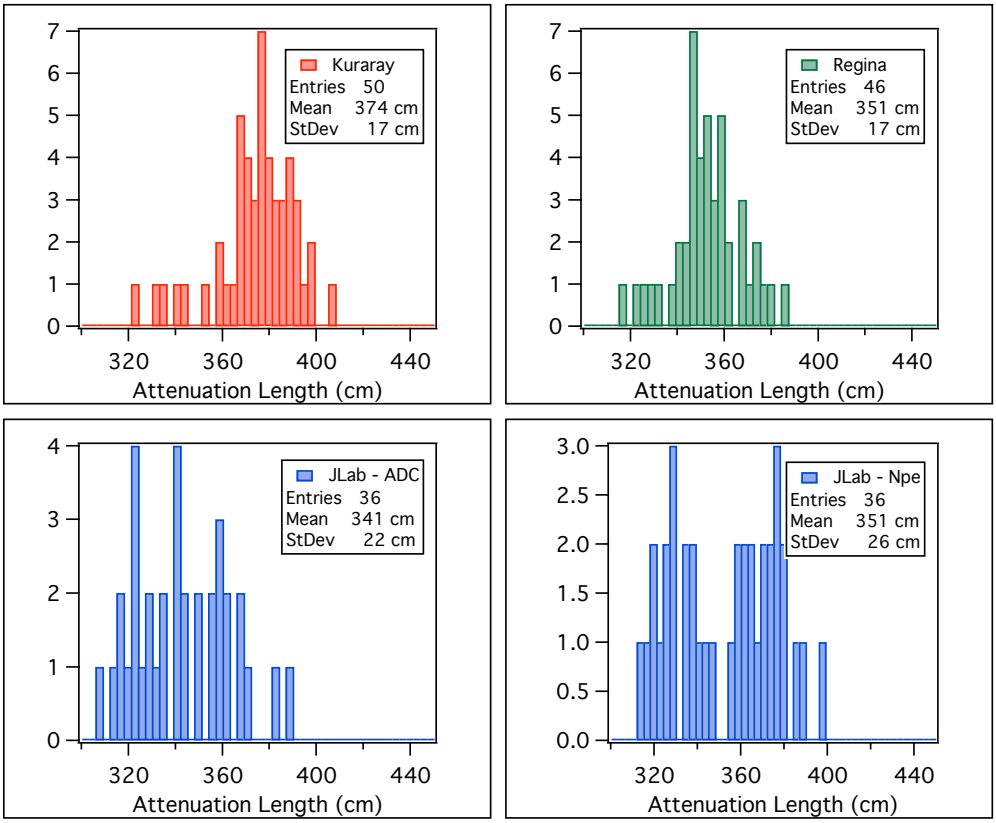


Fig. 13. The attenuation length data sets are shown as histograms for Kuraray, JLab and Regina, respectively.

was $(374 \pm 17)$ cm. It is noteworthy that the Regina standard deviation is in agreement with that of Kuraray's "opposite end blackened" method, with the JLab $N_{pe}$ distribution being wider by a factor of 1.5. A similar trend was observed by Kuraray, with the rough cut measurements having a larger standard deviation by a factor of 1.8 [9].

The Regina average is in agreement with the JLab $N_{pe}$ and 3% higher than JLab's ADC number, although all results agree within error. The small systematic difference between the two JLab results is most likely due to the sensitivity in fitting the $N_{pe}$ spectra, whereas the ADC-based number tracks in a simpler fashion to the length scan, if the ADC scale is linear over its entire range. The Regina ADC was examined and a small non-linearity is present at low ADC values. The slightly different end treatment between Regina and JLab should not contribute significantly. Kuraray has shown that the "Kuraray" method (no treatment of far end) yields higher attenuation length than the "opposite end blackened" method [9], although when both end types are blackened, as is the case for both Regina and JLab fibres, the difference should be small. Regina and JLab measurements have confirmed this.

Finally, the Regina results are also $\sim 5\%$ lower than Kuraray's, for the same style of end treatment, although it should be stressed that the results are in agreement statistically with each other within $1\sigma$. The Hamamatsu S2281 photodiode used by Regina has a flat quantum efficiency response in the 425-700 nm range, with the QE rising gently over this range. In principle, such a response tends to favour wavelengths having longer attenuation lengths than those promoted by a bi-alkali PMT such as the Hamamatsu R647 that Kuraray employed. This is not what is observed here based on a comparison of the means alone. If any systematic differences exist, they are likely to be small.

### *8.2 Number of photoelectrons*

The light output from both Kuraray methods is histogrammed in Fig. 14. It should be noted that since Kuraray extracts the light output in units of $mV$ whereas the GlueX Collaboration measures number of photoelectrons, an absolute comparison is not possible. The histograms are presented here simply to support the statement that the "Kuraray" method yields more light than the "opposite end blackened" method, by on average 17%.

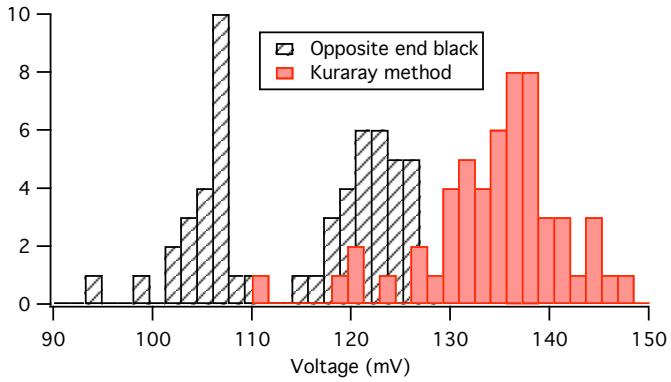


Fig. 14. The fibre light output is shown, as measured by Kuraray using their two methods with the source at 200 cm. Details can be found in the text.

In the end, 46 of the Regina fibres were used in order to extract the number of photoelectrons resulting from the $^{90}Sr$ radioactive source excitation of the fibre's core material and using the PMT as the photosensor. The results yield a mean extracted number of photoelectrons $\zeta = 7.1 \pm 0.7$. In a similar fashion, 40 fibres were tested at JLab resulting in $\zeta = 6.1 \pm 0.7$, about 14% lower than the Regina value owing mostly to lack of optical-grease coupling between the near fibre end photosensor in the JLab tests. The results from both sets exceed the contract specifications of greater than 3.5 with an RMS of 15%.

## 9 Summary and Conclusions

The objective of this study was to characterize the Kuraray SCSF-78MJ scintillating optical fibres, namely the diameter uniformity, the spectral shape, bulk attenuation length, and the number of photoelectrons [11] . The specifications and results are summarized below:

- **Diameter.** *Specifications:* Dimensional uniformity of the diameter was specified at 1 mm with a $RMS \leq 2\%$. *Measurements:* The diameter was measured at three lengths across each fibre (50 cm, 200 cm and 350 cm) and was found to be $(1.002 \pm 0.006)$ mm ($RMS \leq 0.6\%$).
- **Spectral shape.** The spectral shape was measured using a spectrophotometer and was as expected, based on past measurements and experience of similar types of fibres.
- **Effective attenuation length.** *Specifications:* greater than 300 cm when measured with a bi-alkali photomultiplier tube and with $RMS \leq 10\%$. *Measurements:* The effective attenuation length was extracted to be $(351 \pm 17)$ cm ($RMS \leq 5\%$) using a photodiode, and $(341 \pm 22)$ cm to $(351 \pm 26)$ cm using a PMT, and on both cases by fitting over the 100-280 cm source distance range with a single exponential function..
- **Light output.** *Specifications:* This is quantified by the GlueX Collaboration as the number of photoelectrons collected at the fibre's end and must be greater than 3.5 p.e. using a bi-alkali PMT at 200 cm from the source and with $RMS \leq 15\%$. *Measurements:* The mean extracted number of photoelectrons at 200 cm was found to be $7.1 \pm 0.7$ ($RMS < 10\%$) from the Regina data and $6.1 \pm 0.7$ ($RMS < 12\%$) from the JLab data, both employing standard vacuum PMTs.

Clearly, all tested fibres meet or exceed the contract specifications to Kuraray.

## 10 Acknowledgments

This work was supported by NSERC grant SAPJ-326516 and DOE grant DE-FG02-0SER41374 as well as Jefferson Science Associates, LLC. under U.S. DOE Contract No. DE-AC05-06OR23177. We wish to thank Kuraray for providing us with their past cummulative data in addition to their measurements of these first article fibres.

[11] Additional requirements specifying the characteristics of cladding thickness, time structure and base material components, were not evaluated.

## A Fibre Condition

Among the tested fibres, four exhibited evidence of a crack, break or other defect, as shown in Fig. A.1: fibres 3-2, 3-9 and 3-49. These fibres were tested early on, before the experimental setup had been finalized, and as a result damage due to handling at Regina can not be excluded. The extracted attenuation lengths from these three fibres were excluded from the results reported in Section 8 for this reason. A fourth fibre (3-48) was broken after the initial measurement, and is included in the data set.

A fifth fibre (2-2) was suspected as having damage, based on visual inspection, but had no obvious "kink" in its attenuation length data. However, this fibre yielded the lowest number of photoelectrons, approximately 4 (see Section 7). Repeated re-coupling and re-testing of this fibre did not inprove its mean number of photoelectrons, but nevertheless was kept in the data set.

New handling procedures were developed and implemented for the tests of production fibres. The new procedures greatly reduced the change of damaging fibres as evidenced by the fact that only two fibres have been found to have defects out of more than 300 tested from the production fibre batches.

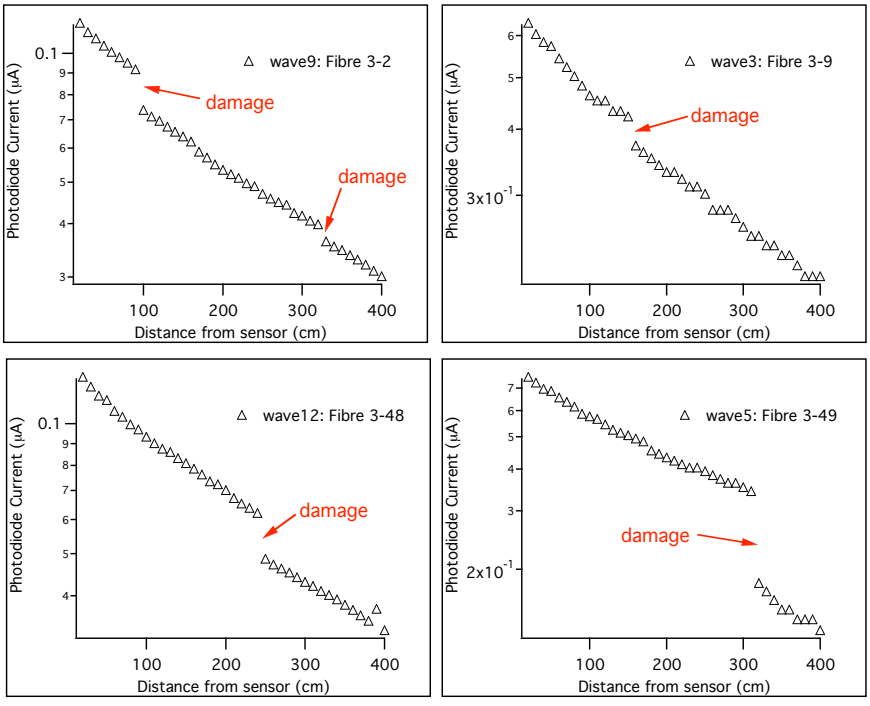


Fig. A.1. Four fibres exhibited signs of a defect or break, with the location is indicated on the plots. These fibres were tested early on, before the setup had been finalized, and as a result damage due to handling at Regina can not be excluded.

## B Treatment of fibre ends

### *B.1 Regina Tests*

The attenuation length of selected fibres was extracted based on different treatment of the ends. The data are shown in Fig. B.1 for a sample fibre and the respective attenuation lengths in the 100-280 cm range of fitting were as follows:

- far end: polished, blackened; near end: grease - $(351 \pm 7)$ cm,
- far end: polished, not blackened; near end: grease - $(363 \pm 7)$ cm,
- far end: rough cut, not blackened; near end: grease - $(385 \pm 9)$ cm,
- far end: polished, blackened; near end: no grease - $(348 \pm 8)$ cm,

with the near end always polished. As claimed above, the attenuation length behaves as expected with the rough-cut and polished-unblackened ends having progressively longer attenuation lengths than the polished-blackened ones, by 8-9% and 6%, respectively. Blackening the rough cut decreases the attenuation length by about 8%. Absence of optical grease between the near end and photo sensor reduces the overall intensity along the length scan by up to 10%, without noticeably affecting the attenuation length extracted from fitting the 100-280 cm range. *To summarize, Regina used polished-blackened far ends, JLab left the far fibre ends untreated (factory cut), while Kuraray measured both with rough-cut and polished/blackened far ends.*

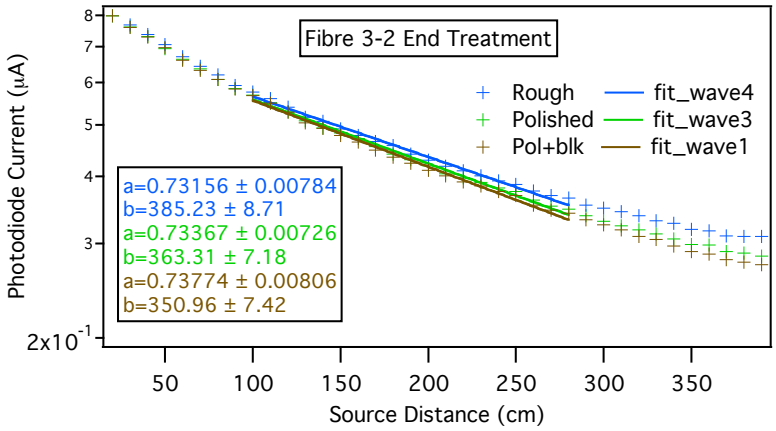


Fig. B.1. The comparison of fibre far end treatment for fibre 3-2 is graphed. The legend is self explanatory. In all cases the near end was polished and coupled to the photodiode with optical grease.

The fibre end that is coupled to the FPM was polished while the other end was left as received from the manufacturer. "Secondary light", reflected at the other end of the fibre and travel back through the fibre, can be detected by the FPM, depending on the $^{90}Sr$ source location. If the $^{90}Sr$ source is positioned at 50 cm from the FPM, the secondary light is not detected, due to the combination of total length traveled and the ADC gate setting. However, if the $^{90}Sr$ source is located near the far end, this light is detected.

Several tests were performed to test these expectations. In a first test the scan was done once with the untreated end and then repeated with the end painted black. This test was done for eight fibres. All measurements confirmed the above assumption. If the source is positioned far away from the FPM the effect is the largest and the measured light output is significantly smaller when the other end of the fibre is painted black. The maximum effect is a 10% reduction in the mean number of photoelectrons when the $^{90}Sr$ source is positioned at 320 cm from FPM and the free fibre end is pained black, in agreement with the Regina tests (see Section B.1). At the center of the fibre this effect is about 5%. The effect on the attenuation length that was extracted from the data by a fit to the data using an exponential function will be dominated by the data points farthest away from the FPM resulting in an attenuation length that is about 10% smaller when the fibre end is painted black. The effect is very reproducible and consistent between the tested eight fibres.

One fibre was subjected to three additional scans where the fibre end was first cut with a knife then polished and then painted black. After each treatment a scan was performed. The results are qualitatively similar to those shown in the left panel of Fig. B.1. The main effect is a reduction in the light output dominated by painting the fibre end black. It does not matter if the painted fibre end had been polished first. However, there is a difference between polished and unpolished fibre end if it is not painted black. In summary, the effect of treating the fibre is dominated by painting it black and is the largest the farthest away the light source is from the readout PMT and amounts to about 10% in terms of the light output.

## References


[1] Jefferson Lab Contract to Kuraray, Specification No. D00000-01007-S001.

[2] GlueX/Hall D Collaboration, The Science of Quark Confinement and Gluonic Excitations, GlueX/Hall D Design Report, **Ver.4** (2002). (http://www.phys.cmu.edu/halld).

[3] A.R. Dzierba, C.A. Meyer and E.S. Swanson, American Scientist, **88**, 406 (2000).

[4] A.J. Davis *et al.*, Nucl. Instr. and Meth. A 276 (1989) 347.

[5] Yu.G. Kudenko, L.S. Littenberg, V.A. Mayatski, O.V. Mineev and N.V. Yershov, Nucl. Instr. and Meth. A 469 (2001) 340.

[6] C.P. Achenbach, arXiv:nucl-ex/0404008 v1, (2004).

[7] Z. Papandreou, B.D. Leverington, G.J. Lolos, Nucl. Instr. and Meth. A 596 (2008) 338.

[8] Z. Papandreou *et al.*, "Report on the First and Second Shipments of Kuraray SCSF-78MJ Production Fibres for the GlueX Barrel Calorimeter", *in preparation.*

[9] Kuraray, "Standard Reference Fibers" of SCSF-78MJ for Jlab and Regina, February 20, 2009.

[10] Kuraray Scintillation Materials broschure (October 2006).

[11] K. Janzen, A. Semenov, G.J. Lolos and Z. Papandreou, GlueX-doc-1178-v1 (http://portal.gluex.org/, Documents, Public), Technical Report, GlueX Collaboration, 2008.

[12] A. Fasso, A. Ferrari, J. Ranft, P.R. Sala, "FLUKA: a multi-particle transport code", CERN-2005-10 (2005), INFN/TC05/11, SLAC-R-773.

[13] I. Chirikov-Zorin et al. Nucl. Instrum. Meth. A456, 310 (2001).

[14] R. Bollmann et al. Nucl. Instrum. Meth. A342, 466 (1994).